Hindawi Publishing Corporation
Journal of Nanomaterials
Volume 2015, Article ID 890637, 7 pages
http://dx.doi.org/10.1155/2015/890637

Research Article

Electronic Tongue Based on Nanostructured Hybrid Films of Gold Nanoparticles and Phthalocyanines for Milk Analysis

Luiza A. Mercante,[1] Vanessa P. Scagion,[1,2] Adriana Pavinatto,[1] Rafaela C. Sanfelice,[1] Luiz H. C. Mattoso,[1] and Daniel S. Correa[1,2]

[1] *National Laboratory for Nanotechnology in Agribusiness (LNNA), Embrapa Instrumentation, 13560-970 São Carlos, SP, Brazil*
[2] *Center for Exact Sciences and Technology, Federal University of São Carlos (UFSCar), 13565-905 São Carlos, SP, Brazil*

Correspondence should be addressed to Luiza A. Mercante; lamercante@gmail.com
and Daniel S. Correa; daniel.correa@embrapa.br

Received 29 September 2015; Accepted 25 October 2015

Academic Editor: David Cornu

The use of gold nanoparticles combined with other organic and inorganic materials for designing nanostructured films has demonstrated their versatility for various applications, including optoelectronic devices and chemical sensors. In this study, we reported the synthesis and characterization of gold nanoparticles stabilized with poly(allylamine hydrochloride) (Au@PAH NPs), as well as the capability of this material to form multilayer Layer-by-Layer (LbL) nanostructured films with metal tetrasulfonated phthalocyanines (MTsPc). Film growth was monitored by UV-Vis absorption spectroscopy, atomic force microscopy (AFM), and Fourier transform infrared spectroscopy (FTIR). Once LbL films have been applied as active layers in chemical sensors, Au@PAH/MTsPc and PAH/MTsPc LbL films were used in an electronic tongue system for milk analysis regarding fat content. The capacitance data were treated using Principal Component Analysis (PCA), revealing the role played by the gold nanoparticles on the LbL films electrical properties, enabling this kind of system to be used for analyzing complex matrices such as milk without any prior pretreatment.

1. Introduction

During the past few years, hybrid nanomaterials have been widely used for several kinds of applications such as the development of chemical sensors [1–4] and biosensors [5–7]. Although there are many methods for producing such materials, strong emphasis has been given on the fabrication techniques that allow the precise control of molecular architectures, including the Langmuir-Blodgett (LB) and Layer-by-Layer (LbL) methods [8]. The LbL technique [9] is probably the most commonly used technique owing to its efficiency and molecular architecture control, combined with its experimental simplicity and low cost [10]. Besides the architecture of the film, the choice of the materials is also important to determine the film final properties. Among the many possible materials, gold nanoparticles have been used once they present high surface area and electrical conductivity and catalytic properties that make them excellent materials for the detection of a wide range of analytes [11, 12]. However, the use of gold nanoparticles for improving the electrical properties of LbL films in chemical sensor arrays, such as electronic tongues, has not received much attention.

In this study we focus on nanostructured architectures whose properties are varied significantly by the interplay among the constituent materials. Specifically, here we report the synthesis of gold nanoparticles functionalized with poly(allylamine hydrochloride) and its use for the fabrication of LbL films with copper and nickel tetrasulfonated phthalocyanines. We use the functionalized nanoparticles to enhance the electrical properties of the LbL films, which were applied in chemical sensing experiments using an electronic tongue (e-tongue) system. The e-tongue was composed of an array of platinum interdigitated electrodes coated with LbL films of distinct compositions and used to analyze milk samples via impedance spectroscopy technique. The electronic tongue was able to distinguish milks with different fat contents, showing the practical utility of the employed approach.

2. Experimental

2.1. Materials. Copper(II) tetrasulfonated phthalocyanine (CuTsPc), nickel(II) tetrasulfonated phthalocyanine (NiTsPc), poly(allylamine hydrochloride) (PAH, $M_w = 17.500$), sodium borohydride ($NaBH_4$), and tetrachloroauric(III) acid ($HAuCl_4$) were purchased from Sigma-Aldrich and used as received. Platinum interdigitated electrodes (IDEs), each one comprising 50 pairs of fingers with finger width and distance between fingers of 10 μm, were designed to exhibit a capacitive profile. The IDEs were fabricated by photolithography at the Brazilian Nanotechnology National Laboratory (LNNano-LNLS).

2.2. Synthesis of Au@PAH Nanoparticles. Gold nanoparticles were synthetized following the procedure described previously by Alencar et al. [13]. 1.0 mL of aqueous $NaBH_4$ solution (10^{-2} mol L^{-1}) was added dropwise under vigorous stirring to a HCl solution (pH 3) containing 1.0 mL PAH (10^{-2} mol L^{-1}) and 1.0 mL $HAuCl_4$ (10^{-3} mol L^{-1}). The stoichiometric ratio of $NaBH_4$ and $HAuCl_4$ was kept at 10 to ensure total reduction of Au^{3+} to Au^0. After 30 min, the reaction was complete, with the aqueous solution containing Au@PAH NPs displaying a reddish color, characteristic of gold nanoparticles formation.

2.3. Preparation of LbL Films. Solutions of 1 mg mL^{-1} of Au@PAH NPs, PAH, CuTsPc, and NiTsPc were prepared by dispersing the materials in HCl aqueous solution (pH 3). LbL films were deposited on quartz, silicon, and platinum interdigitated electrodes substrates by alternating immersion into cationic (Au@PAH NPs and PAH) and anionic (CuTsPc and NiTsPc) solutions. PAH/CuTsPc, PAH/NiTsPc, Au@PAH/CuTsPc, and Au@PAH/NiTsPc LbL films were prepared varying the number of bilayers by immersing the substrate for 30 min in the Au@PAH NPs solution and for 5 min into the PAH or phthalocyanines solutions.

2.4. LbL Film Characterization. The morphology and thickness of LbL films adsorbed on glass substrates were assessed by AFM using a Dimension V (Veeco) microscope. All images were obtained in the Tapping mode with a scan rate of 0.6 Hz, using silicon nitride tips attached to a cantilever of spring constant of 2.5 N m^{-1}. The root-mean square roughness (R_{rms}) was calculated using Gwydion 2.1 data analysis software. The UV-Vis absorption spectra were recorded using a Perkin-Elmer Lambda 25 on quartz slides. FTIR spectroscopy was performed on a Perkin-Elmer 1000 using silicon wafers as substrates for the films. A total of 64 scans were collected at a resolution of 2 cm^{-1}.

2.5. Milk Samples. Twenty-four milks from distinct commercial brands with different fat contents were purchased from a local supplier. The 24 samples included 10 fat, 7 semi-skimmed, and 7 skimmed milk samples. The milk samples were prepared by adding 100 μL of each milk sample to 100 mL of phosphate buffer (pH = 6.5), which were analyzed by the e-tongue system without any prior pretreatment.

2.6. Electrical Measurements. Impedance spectroscopy measurements of milk samples using the e-tongue were carried out with a Solartron analyzer (model 1260A). All measurements were carried out in phosphate buffer solutions (pH = 6.5) and the data were collected in the range from 1 Hz up to 1 MHz, with an *ac* applied voltage of 50 mV. The sensor array composing the e-tongue was comprised of three sensing units: a bare platinum interdigitated electrode and two electrodes coated with 7-bilayer LbL film of PAH/CuTsPc and PAH/NiTsPc (named e-tongue 1). For comparison and in order to investigate the effect of gold nanoparticles on the electrical performance of the LbL films, electrodes coated with 7-bilayer LbL film of Au@PAH/CuTsPc and Au@PAH/NiTsPc were also prepared (named e-tongue 2). The electrodes were left soaked into the solutions for 20 min prior to the start of the electrical measurements. Five independent acquisitions using the two e-tongues were carried out for each milk sample. By carefully washing the sensing units with deionized water to remove possible molecules entrapped within the films, the sensors could be reused in further experiments. Electrical measurements in phosphate buffer solution before and after exposing the sensing units to the milk samples yielded similar results (data not shown), indicating that sensor contamination was negligible, reinforcing the reusability of the sensor. The capacitance values obtained were treated using the statistical method known as Principal Component Analysis (PCA), which correlates samples by decreasing the dimensionality of the original data without losing relevant information. Briefly, PCA makes a linear combination of the data, creating another pair of orthogonal axes into the directions where the higher correlations exist [14].

3. Results and Discussion

3.1. Synthesis of Au@PAH Nanoparticles. For the synthesis of gold nanoparticles, $NaBH_4$ is employed as the reducing agent of gold ions. However, once $NaBH_4$ is not a strong stabilizing agent for the nanoparticles, PAH was used as stabilizer in order to prevent nanoparticle agglomeration and precipitation [13]. The Au@PAH NPs formed display a surface plasmon resonance (SPR) absorption band centered at 520 nm, according to the UV-VIS spectrum (Figure 1(a)) and spherical shape with a mean diameter of 11 nm, as shown in the TEM image (Figure 1(b)).

The colloidal stability of Au@PAH nanoparticles was analyzed by two parameters, the hydrodynamic diameter and zeta potential. The first parameter is associated with the fact that when the nanoparticles are not stable in solution, they tend to agglomerate, yielding higher values of diameters. The zeta potential is related to the effective charge of the particles. The higher the absolute potential value, the higher the stability of the colloidal system, once the charged particles tend to repel each other and therefore overcome the natural tendency of aggregation. Before measuring the colloidal stability of Au@PAH nanoparticles, the dispersion was filtered through a

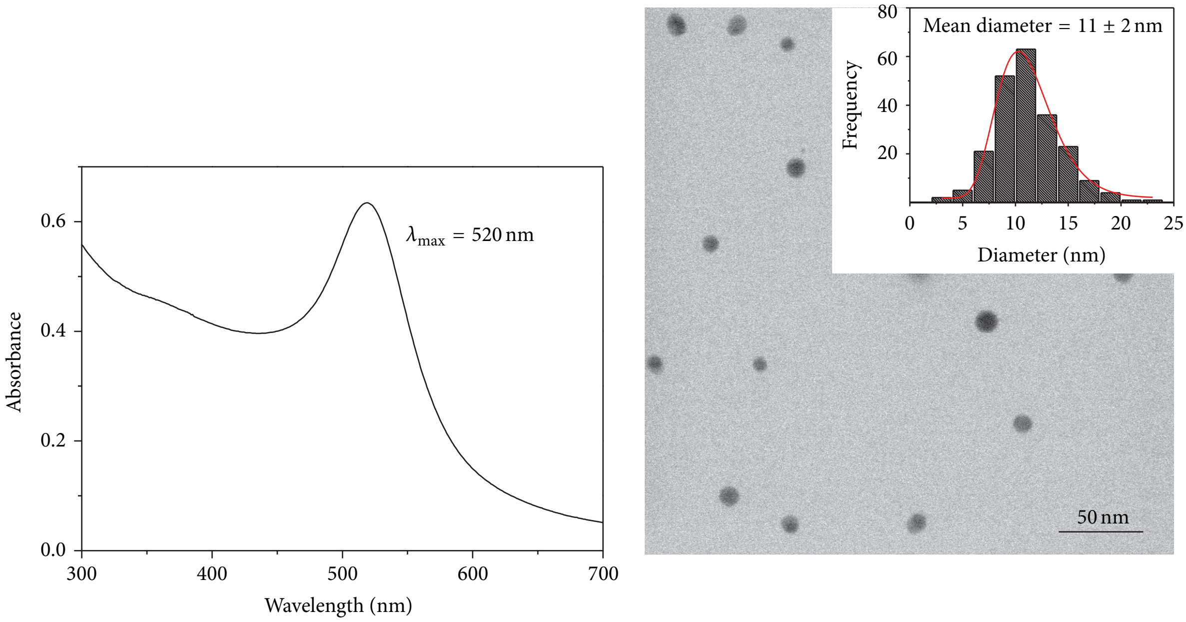

(a)

(b)

Figure 1: (a) UV-Vis absorption spectrum and (b) TEM image of Au@PAH nanoparticles. The inset in (b) shows the histogram of size distribution.

membrane having pore size of 0.22 μM. The values found for the hydrodynamic diameter and zeta potential were 22 nm and 29 mV, respectively, confirming the stability of the synthesized nanoparticles. The positive value of the zeta potential is related to positive charge of PAH due to the protonation of the amino group in the polymer chain. The hydrodynamic diameter value close to the nanoparticles diameter obtained by TEM images (Figure 1(b)) demonstrates that PAH acts as a stabilizer avoiding the agglomeration of the nanoparticles. This information is important because it allows such nanoparticles to be used in the fabrication of LbL films, as will be discussed in the following section.

3.2. LbL Films Characterization. Nanostructured LbL films have been widely used as active layers in sensors and biosensors platforms, once they are one of the main approaches used to fabricate highly organized and morphologically controlled nanostructures at molecular level [15–17]. The LbL films architectures were built on quartz substrate and the sequential growth was monitored by UV-Vis absorption spectroscopy, as shown in Figure 2, for films formed by Au@PAH/CuTsPc (Figure 2(a)) and Au@PAH/NiTsPc (Figure 2(b)). The spectra show two distinct absorption regions, one in the visible and the other in the ultraviolet range, assigned to π-π^* electronic transitions from macrocyclic ring of phthalocyanine, referenced as Q and B bands, respectively [18]. More specifically, Q bands arise due to electronic transitions from electrons in the outer rings while B bands arise from electrons in both inner and outer rings [18]. The Q band comprises two different peaks displaying a maximum of absorption: at 617 nm (Figure 2(a)) and 619 nm (Figure 2(b)) assigned to the absorption of dimmers and higher order of aggregates and at 669 nm (Figure 2(a)) and 667 nm (Figure 2(b)) related to the monomers absorption [19]. The B bands are centered around 340 nm for both films and the other absorption regions are attributed to the metal compound in the center of the phthalocyanine structures as reported by Edwards and Gouterman [20]. It is worth noting that the band at 520 nm assigned to the gold nanoparticles surface plasmon resonance could not be observed in the UV-Vis absorption spectra due to the overlapping with Q bands from phthalocyanines and also the low amount of the nanoparticles in the films [13].

A linear growth was observed for the film formed by Au@PAH/CuTsPc (inset of Figure 2(a)). The absorbance at 617 nm increased linearly with the number of bilayers, which indicates that the same amount of material was adsorbed for each bilayer deposition. Similar results were reported by Alencar et al. and Silva et al. [13, 21]. However, Au@PAH/NiTsPc film (from 1 to 7 bilayers) presented two linear regions for film growth, as can be observed in the inset of Figure 2(b): one ranging from 1 to 3 bilayers and the other from 3 to 7 bilayers, as displayed. This result suggests reorganization of the materials in the films from the third bilayer leading to irregular (increase) amount of material adsorbed, which can be attributed, for instance, to NiTsPc diffusion/interaction into Au@PAH layers [22].

FTIR measurements were performed in order to investigate the adsorption and supramolecular interaction between the components of the films. Figure 3 shows the spectra for 15-bilayer LbL films formed by Au@PAH/CuTsPc (Figure 3(a)) and Au@PAH/NiTsPc (Figure 3(b)), where the characteristics bands for PAH and phthalocyanines can be viewed in both spectra. The main bands of phthalocyanines are assigned at 1032 and 1034 cm^{-1} (S-O stretching vibration

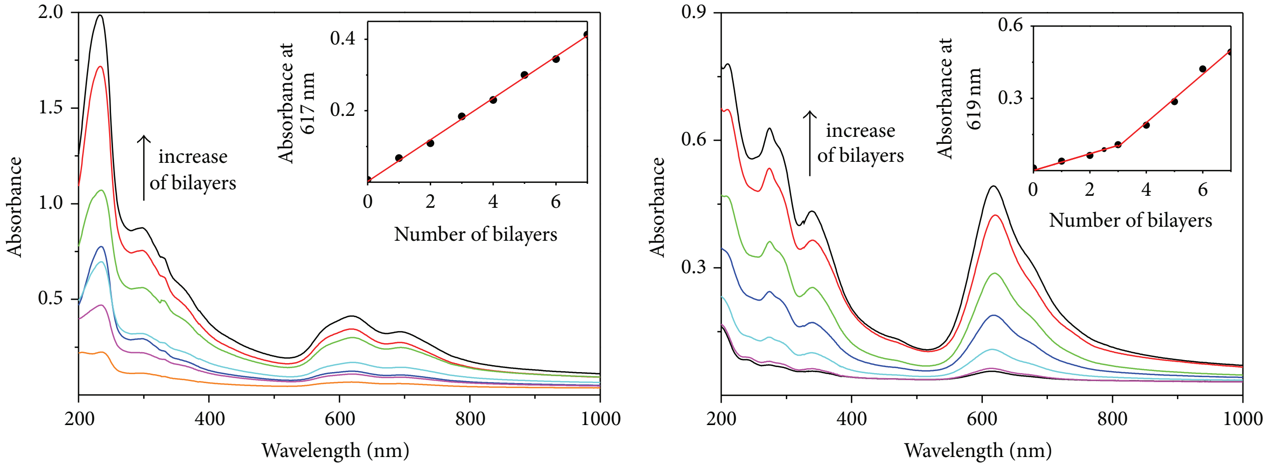

(a) (b)

Figure 2: UV-Vis absorption spectra for LbL films ranging from 1 up to 7 bilayers of (a) Au@PAH/CuTsPc and (b) Au@PAH/NiTsPc. The inset shows the absorbance at (a) 617 nm and (b) 619 nm versus number of bilayers for respective architectures.

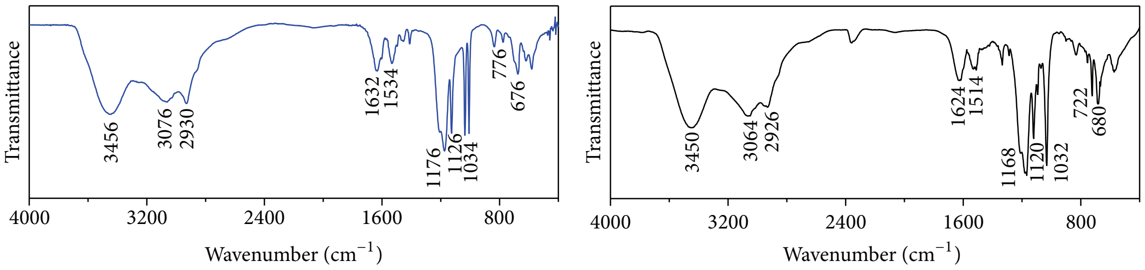

(a) (b)

Figure 3: FTIR spectra in the transmission mode for 15-bilayer LbL films of (a) Au@PAH/CuTsPc and (b) Au@PAH/NiTsPc.

deformation), 1120 and 1126 cm^{-1} (S=O symmetric stretching), and 1624 and 1632 cm^{-1} (C=C axial stretching from aromatic ring). The bands at 1120 and 1130 cm^{-1} (C-N angular deformation) and 1514 and 1534 cm^{-1} (C-N axial deformation) and the bands in the range of 2926–3076 cm^{-1} (C-H axial deformation) can be assigned to both materials, while the strong bands at 3450 and 3456 cm^{-1} are related to the stretching mode of the $\mathrm{NH_3}^+$ from PAH [13, 18]. The bands assigned to S-O stretching are shifted to low energies in the LbL films in comparison with FTIR spectra for CuTsPc [23] and NiTsPc [13] cast films. These findings suggest interaction at supramolecular level between the $\mathrm{SO_3}^-$ group of phthalocyanines and $\mathrm{NH_3}^+$ group of PAH, which leads to the formation of the "salt-bridge" reported in the literature [13, 18, 23].

The film morphology was investigated by AFM technique using the 7-bilayer LbL films of Au@PAH/CuTsPc and Au@PAH/NiTsPc, as shown in Figures 4(a) and 4(b). Higher roughness (R_{rms}) was observed for Au@PAH/NiTsPc (R_{rms} = 16.8 nm) film compared to Au@PAH/CuTsPc (R_{rms} = 8.3 nm), which suggests interpenetration of the NiTsPc in the Au@PAH during the film formation. These findings corroborate the difference observed on film growth as shown in the UV-Vis spectra (Figure 2).

3.3. Electrical Properties. Before using the IDEs modified with the LbL films as the sensing units of the e-tongue system, several measurements were performed with the bare platinum electrodes immersed in distilled water to guarantee similar electrical responses. Therefore, any minor changes observed in the impedance data, after the deposition of the LbL films, are in fact due to the difference between the samples, instead of subtle changes attributed to the design of the electrodes [24]. Capacitance measurements at 1 kHz were performed on the platinum electrodes coated with the LbL films as shown in Figure 5. The frequency of 1 kHz was chosen to analyze the data because normally higher sensitivity is achieved at lower frequencies owing to the importance of the electrical double-layer in the electrical response [25]. In order to evaluate the influence of the gold nanoparticles on the sensing properties of the nanostructured architectures, the LbL films without gold nanoparticles were fabricated and also used for capacitance measurements.

From Figure 5, it is clear that the sensing units containing Au@PAH NPs were able to differentiate the milk samples and displayed an increase in the capacitance values at 1 kHz as the fat content increases in the sample. These shifts in the capacitance values are stronger in the LbL films containing the gold nanoparticles, revealing that the gold nanoparticles increase

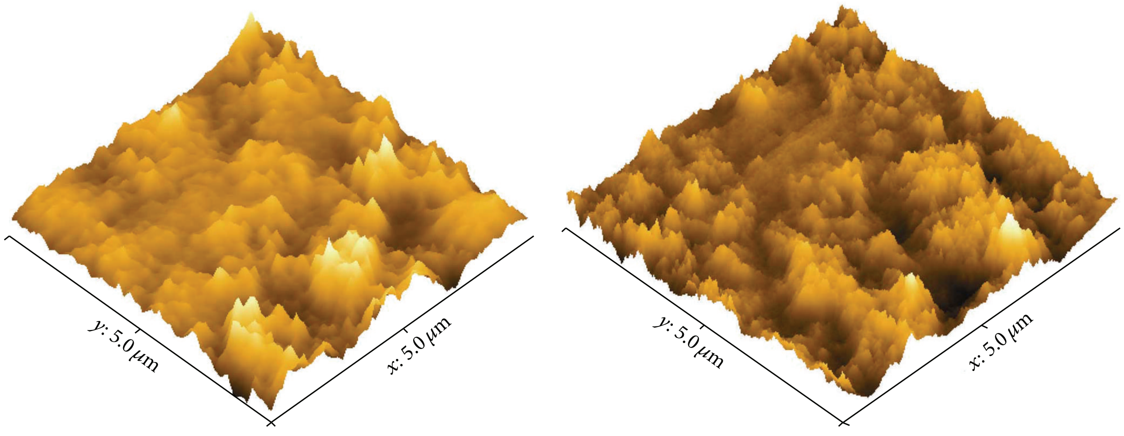

(a)

(b)

Figure 4: AFM 3D images of 7-bilayer LbL films of (a) Au@PAH/CuTsPc and (b) Au@PAH/NiTsPc.

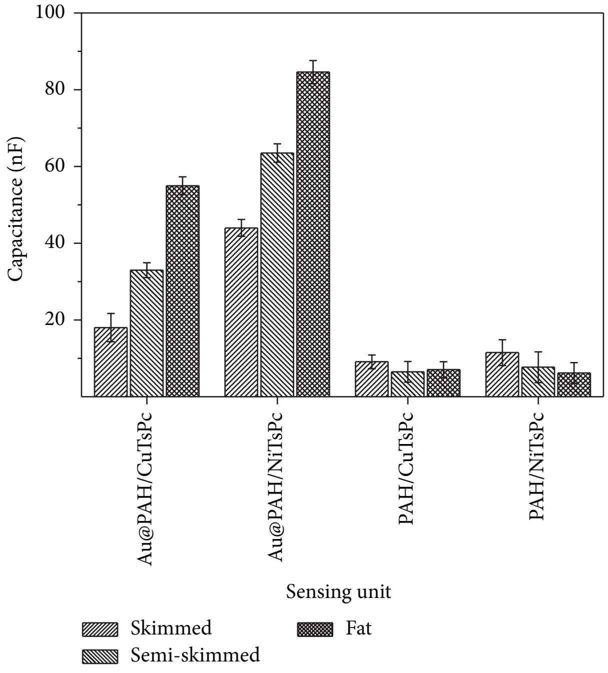

Figure 5: Capacitance measurements of fat, skimmed, and semi-skimmed milk samples at 1 kHz for the four different sensing units containing 7-bilayer LbL films of Au@PAH/CuTsPc, Au@PAH/NiTsPc, PAH/CuTsPc, and PAH/NiTsPc.

the efficiency of the LbL films as sensing platforms. Possibly, this improvement is due to the good electrical conductivity and the capability of nanoparticles to enhance the electrical contact of the sample molecules with the electrode surface [12].

It is known that the limit of detection of an array of sensors is often lower than that of a single sensor [26]. Therefore, to test the ability of an electronic tongue to classify milk samples, its sensing units (including the blank electrode) formed by interdigitated electrodes modified with 7-bilayer films of PAH/CuTsPc and PAH/NiTsPc (e-tongue 1) were immersed into a set of 24 milk samples (10 fat, 7 skimmed, and 7 semi-skimmed commercial milk samples), and electrical capacitance data at 1 KHz and 50 mV were collected to be used in the PCA analysis. The results in Figure 6(a) show that e-tongue 1 could not satisfactorily distinguish the distinct milk samples, where no correspondence in the data could be related to the principal components. On the other hand, the discriminating capability of the sensor array composed of sensing units with Au@PAH NPs (e-tongue 2) is more evident, as illustrated in the PCA plot of Figure 6(b). For instance, we note that fat milk samples were located on the positive side of PC1. Skimmed milks can be seen in a cluster located on the negative side of PC1 and positive side of PC2, while almost all semi-skimmed milk samples are grouped on the negative sides of PC1 and PC2. Only two samples of semi-skimmed milks are located close to skimmed milks, probably due to the lower fat content for these samples, since semi-skimmed samples can present a range of fat content (1-2%). Moreover, the data variance was mainly accounted using two first principal components, yielding 78% (PC1 + PC2) of the total information collected by the array.

It is worth mentioning that the measurements presented here were carried out using LbL films with a fixed number of bilayers (seven), and therefore no attempt was made to investigate possible effects of the number of film layers on the sensor sensitivity. However, previous studies have demonstrated that sensor optimal performance can usually be attained using from 5-bilayer to 10-bilayer films because they are sufficiently thin to increase sensitivity while providing full coverage of the electrodes, which may not occur for very thin films [27].

4. Conclusion

Gold nanoparticles functionalized with PAH with an average diameter of 11 nm were synthetized and used to grow nanostructured LbL films containing metal tetrasulfonated phthalocyanines. These LbL films were used to modify interdigitated platinum electrodes and were applied as sensing units

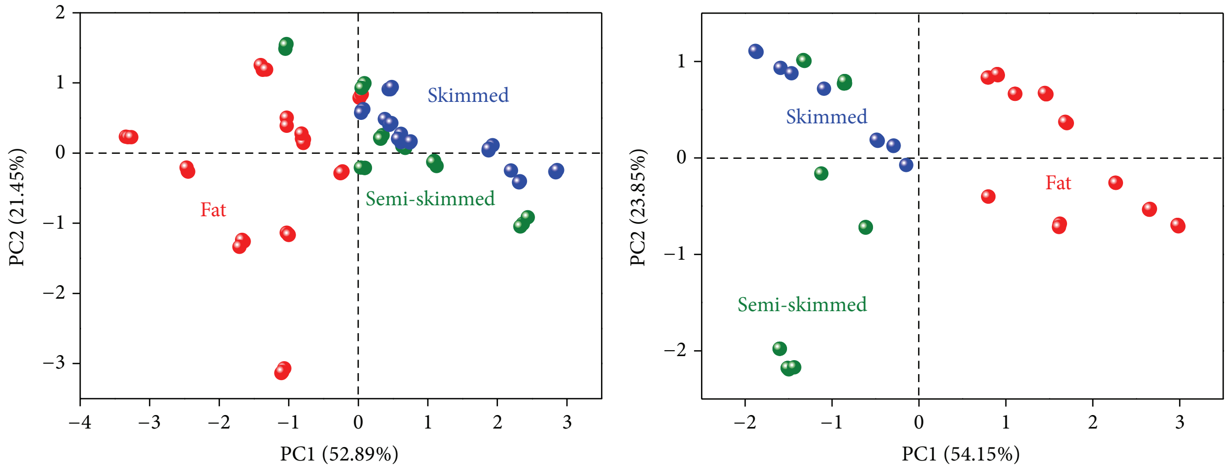

(a)

(b)

Figure 6: PCA plots for milk samples obtained from electrical capacitance values recorded at 1 kHz and 50 mV for two different e-tongues comprising 3 sensing units each, as follows: (a) e-tongue 1: bare electrode and 7-bilayer PAH/CuTsPc and 7-bilayer PAH/NiTsPc LbL films and (b) e-tongue 2: bare electrode and 7-bilayer Au@PAH/CuTsPc and 7-bilayer Au@PAH/NiTsPc LbL films. The data variance for PC1 and PC2 is included in the figure.

of an electronic tongue sensor aiming to distinguish milk samples with different fat contents. The presence of the Au@PAH NPs in the LbL films increased the sensor sensitivity when compared to the films without nanoparticles, as shown by the PCA method, revealing that the presence of gold nanoparticles greatly improves the conductivity of the film and enhances the sensitivity of the e-tongue. The results presented here demonstrate that gold nanoparticles can be used to modify LbL films to produce sensing units for an electronic tongue with higher sensitivity to evaluate liquid samples. Such approach can be used in the development of novel sensor platforms for measuring milk quality and other complex liquid matrices in a fast and low-cost way.

Conflict of Interests

The authors declare that there is no conflict of interests regarding the publication of this paper.

Acknowledgments

The authors acknowledge the financial support by FAPESP (Grants nos. 2012/23880-3, 2013/26712-7, and 2014/16789-5), CNPq, CAPES, MCTI-SisNano, and Embrapa from Brazil.

References

[1] L. Nicole, C. Laberty-Robert, L. Rozes, and C. Sanchez, "Hybrid materials science: a promised land for the integrative design of multifunctional materials," *Nanoscale*, vol. 6, no. 12, pp. 6267–6292, 2014.

[2] L.-N. Wu, Y.-L. Tan, L. Wang et al., "Dopamine sensor based on a hybrid material composed of cuprous oxide hollow microspheres and carbon black," *Microchimica Acta*, vol. 182, no. 7, pp. 1361–1369, 2015.

[3] L. A. Mercante, A. Pavinatto, L. E. Iwaki et al., "Electrospun polyamide 6/poly(allylamine hydrochloride) nanofibers functionalized with carbon nanotubes for electrochemical detection of dopamine," *ACS Applied Materials & Interfaces*, vol. 7, no. 8, pp. 4784–4790, 2015.

[4] R. S. Andre, A. Pavinatto, L. A. Mercante, E. C. Paris, L. H. Mattoso, and D. S. Correa, "Improving the electrochemical properties of polyamide 6/polyaniline electrospun nanofibers by surface modification with ZnO nanoparticles," *RSC Advances*, vol. 5, no. 90, pp. 73875–73881, 2015.

[5] M. S. Artiles, C. S. Rout, and T. S. Fisher, "Graphene-based hybrid materials and devices for biosensing," *Advanced Drug Delivery Reviews*, vol. 63, no. 14-15, pp. 1352–1360, 2011.

[6] W. Zhang, J. Zheng, C. Tan et al., "Designed self-assembled hybrid Au@CdS core-shell nanoparticles with negative charge and their application as highly selective biosensors," *Journal of Materials Chemistry B*, vol. 3, no. 2, pp. 217–224, 2015.

[7] J. Shen, X. Yang, Y. Zhu, H. Kang, H. Cao, and C. Li, "Gold-coated silica-fiber hybrid materials for application in a novel hydrogen peroxide biosensor," *Biosensors and Bioelectronics*, vol. 34, no. 1, pp. 132–136, 2012.

[8] G. Decher and J. B. Schlenoff, *Multilayer Thin Films: Sequential Assembly of Nanocomposite Materials*, Wiley, Weinheim, Germany, 2003.

[9] G. Decher, "Fuzzy nanoassemblies: toward layered polymeric multicomposites," *Science*, vol. 277, no. 5330, pp. 1232–1237, 1997.

[10] S. Srivastava and N. A. Kotov, "Composite Layer-by-Layer (LBL) assembly with inorganic nanoparticles and nanowires," *Accounts of Chemical Research*, vol. 41, no. 12, pp. 1831–1841, 2008.

[11] K. Saha, S. S. Agasti, C. Kim, X. Li, and V. M. Rotello, "Gold nanoparticles in chemical and biological sensing," *Chemical Reviews*, vol. 112, no. 5, pp. 2739–2779, 2012.

[12] E. Katz, I. Willner, and J. Wang, "Electroanalytical and bioelectroanalytical systems based on metal and semiconductor nanoparticles," *Electroanalysis*, vol. 16, no. 1-2, pp. 19–44, 2004.

[13] W. S. Alencar, F. N. Crespilho, M. V. A. Martins, V. Zucolotto, O. N. Oliveira Jr., and W. C. Silva, "Synergistic interaction between gold nanoparticles and nickel phthalocyanine in layer-by-layer (LbL) films: evidence of constitutional dynamic chemistry (CDC)," *Physical Chemistry Chemical Physics*, vol. 11, no. 25, pp. 5086–5091, 2009.

[14] S. Wold, K. Esbensen, and P. Geladi, "Principal component analysis," *Chemometrics and Intelligent Laboratory Systems*, vol. 2, no. 1–3, pp. 37–52, 1987.

[15] J. R. Siqueira Jr., L. Caseli, F. N. Crespilho, V. Zucolotto, and O. N. Oliveira Jr., "Immobilization of biomolecules on nanostructured films for biosensing," *Biosensors and Bioelectronics*, vol. 25, no. 6, pp. 1254–1263, 2010.

[16] A. Pavinatto, L. A. Mercante, C. S. Leandro, L. H. C. Mattoso, and D. S. Correa, "Layer-by-Layer assembled films of chitosan and multi-walled carbon nanotubes for the electrochemical detection of 17α-ethinylestradiol," *Journal of Electroanalytical Chemistry*, vol. 755, pp. 215–220, 2015.

[17] A. Manzoli, F. M. Shimizu, L. A. Mercante et al., "Layer-by-layer fabrication of AgCl-PANI hybrid nanocomposite films for electronic tongues," *Physical Chemistry Chemical Physics*, vol. 16, no. 44, pp. 24275–24281, 2014.

[18] L. N. Furini, E. Feitosa, P. Alessio, M. H. Shimabukuro, A. Riul Jr., and C. J. L. Constantino, "Tuning the nanostructure of DODAB/nickel tetrasulfonated phthalocyanine bilayers in LbL films," *Materials Science and Engineering C*, vol. 33, no. 5, pp. 2937–2946, 2013.

[19] M. F. Zampa, A. C. F. de Brito, I. L. Kitagawa et al., "Natural gum-assisted phthalocyanine immobilization in electroactive nanocomposites: physicochemical characterization and sensing applications," *Biomacromolecules*, vol. 8, no. 11, pp. 3408–3413, 2007.

[20] L. Edwards and M. Gouterman, "Porphyrins. XV. Vapor absorption spectra and stability: phthalocyanines," *Journal of Molecular Spectroscopy*, vol. 33, no. 2, pp. 292–310, 1970.

[21] J. R. Silva, N. C. de Souza, and O. N. Oliveira Jr., "Adsorption kinetics and charge inversion in layer-by-layer films from nickel tetrasulfonated phthalocyanine and poly(allylamine hydrochloride)," *Journal of Non-Crystalline Solids*, vol. 356, no. 18-19, pp. 937–940, 2010.

[22] J. M. Garza, P. Schaaf, S. Muller et al., "Multicompartment films made of alternate polyelectrolyte multilayers of exponential and linear growth," *Langmuir*, vol. 20, no. 17, pp. 7298–7302, 2004.

[23] V. Zucolotto, M. Ferreira, M. R. Cordeiro, C. J. L. Constantino, W. C. Moreira, and O. N. Oliveira Jr., "Nanoscale processing of polyaniline and phthalocyanines for sensing applications," *Sensors and Actuators B: Chemical*, vol. 113, no. 2, pp. 809–815, 2006.

[24] P. H. B. Aoki, D. Volpati, A. Riul Jr., W. Caetano, and C. J. L. Constantino, "Layer-by-layer technique as a new approach to produce nanostructured films containing phospholipids as transducers in sensing applications," *Langmuir*, vol. 25, no. 4, pp. 2331–2338, 2009.

[25] D. M. Taylor and A. G. MacDonald, "AC admittance of the metal/insulator/electrolyte interface," *Journal of Physics D: Applied Physics*, vol. 20, no. 10, pp. 1277–1283, 1987.

[26] A. V. Legin, A. M. Rudnitskaya, Y. G. Vlasov, C. Di Natale, and A. D'Amico, "Features of the electronic tongue in comparison with the characteristics of the discrete ion-selective sensors," *Sensors and Actuators B: Chemical*, vol. 58, no. 1–3, pp. 464–468, 1999.

[27] M. Ferreira, A. Riul Jr., K. Wohnrath, F. J. Fonseca, O. N. Oliveira Jr., and L. H. C. Mattoso, "High-performance taste sensor made from Langmuir−Blodgett films of conducting polymers and a ruthenium complex," *Analytical Chemistry*, vol. 75, no. 4, pp. 953–955, 2003.